

Wiskott-Aldrich syndrome gene mutations modulate cancer susceptibility in the p53[±] murine model

Marton Keszei^a, Joanna S. Kritikou^a, Deborah Sandfort^a, Minghui He^a, Mariana M.S. Oliveira^a, Hannah Wurzer^{ib}, Raoul V. Kuiper^b, and Lisa S. Westerberg^a

^aDepartment of Microbiology Tumor and Cell biology, Karolinska Institutet, Stockholm, Sweden; ^bDepartment of Laboratory Medicine, Karolinska Institutet, Stockholm, Sweden

ABSTRACT

The Wiskott-Aldrich syndrome protein (WASp) is a key regulator of the actin cytoskeleton in hematopoietic cells and mutated in two severe immunodeficiency diseases with high incidence of cancer. Wiskott-Aldrich syndrome (WAS) is caused by loss-of-function mutations in WASp and most frequently associated with lymphoreticular tumors of poor prognosis. X-linked neutropenia (XLN) is caused by gain-of-function mutations in WASp and associated with acute myeloid leukemia (AML) and myelodysplastic syndrome (MDS). To understand the role of WASp in tumorigenesis, we bred WASp⁺, WASp⁻, and WASp-XLN mice onto tumor susceptible p53^{+/-} background and sub-lethally irradiated them to enhance tumor development. We followed the cohorts for 24 weeks and tumors were characterized by histology and flow cytometry to define the tumor incidence, onset, and cell origin. We found that p53^{+/-}WASp⁺ mice developed malignancies, including solid tumors and T cell lymphomas with 71.4% of survival 24 weeks after irradiation. p53^{+/-}WASp⁻ mice showed lower survival rate and developed various early onset malignancies. Surprisingly, the p53^{+/-}WASp-XLN mice developed malignancy mostly with late onset, which caused delayed mortality in this colony. This study provides evidence for that loss-of-function and gain-of-function mutations in WASp influence tumor incidence and onset.

ARTICLE HISTORY

Received 22 January 2018
Revised 16 April 2018
Accepted 19 April 2018

KEYWORDS

WASp; p53; malignancies; genetic model; immunodeficiency

Introduction


Patients that suffer from primary immunodeficiency are at risk to develop haematological malignancies often associated with Epstein-Barr virus infection and of poor prognosis.¹ The reason for increased cancer risk could be failure of the immune system to eradicate tumors or due to intrinsic failure during myelopoiesis and lymphopoiesis. Mutations in the WAS gene that encodes for the cytoskeletal regulator WASp are associated with two immunodeficiency syndromes, Wiskott-Aldrich syndrome (WAS) and X-linked neutropenia (XLN). WAS is caused by loss-of-function mutations in WASp leading to severe immunodeficiency. The tumor incidence in WAS is estimated to be 13–22% with a median age of onset of 9.5 years and with poor prognosis.^{2,3} WAS patient tumors include non-Hodgkin lymphoma, EBV positive and EBV negative lymphoma, Hodgkin lymphoma, Burkitt lymphoma, and less frequently myelodysplasia, acute lymphoblastic leukemia, myelomonocytic leukaemia, and nonhematopoietic malignancies.^{3–10} XLN is caused by mutations that destroy the auto-inhibitory folding of WASp thereby rendering WASp constitutively active.^{11–15} XLN patients show bone marrow arrest at the promyelocyte stage associated with development of myelodysplastic syndrome and acute myeloid leukemia. This is associated with aberrant

segregation of chromosomes to the daughter cells and impaired cytokinesis during mitosis, leading to increased cell death.^{14–16} Moreover, somatic XLN mutations in WASp correlate with poor prognosis in patients with juvenile myelomonocytic leukemia and the XLN-WASp expressing leukemic clone becomes dominant in these patients.¹⁷

We herein sought to identify the tumor incidence, onset, and cell origin in WAS and XLN. Since no spontaneous tumor development has been observed in WASp⁻ knockout and WASp-XLN knockin mouse colonies, we established a tumor model where WASp mutant strains were bred onto tumor prone Trp53 (p53) deficient mice. As the p53 gene is responsible for maintaining genomic integrity during genotoxic stress, p53 deficient mice develop spontaneous tumors with a high incidence.¹⁸ In p53^{±/-} heterozygous mice, which shows only moderate tumor susceptibility, gamma radiation dramatically reduces the latency of tumor development.^{19–21} Due to irradiation induced mutations, the intact wild type p53 allele is mutated in p53^{+/-} tumors, resulting in loss of heterozygosity (LOH), no functional p53 expression, and tumor growth.¹⁹ Importantly, synergy between p53 inactivation and other mutations lead to the emergence of specific tumor types such as p53 loss in Kras^{G12D} knock-in leads to AML²² or Eμ-myc transgene to B cell lymphomas.²³

CONTACT Lisa S. Westerberg  Lisa.Westerberg@ki.se  Department of Microbiology, Tumor and Cell biology, Karolinska Institutet, Stockholm, Sweden; Marton Keszei  Marton.Keszei@ki.se  Department of Department of Microbiology, Tumor and Cell biology, Stockholm, Sweden

Color versions of one or more of the figures in the article can be found online at www.tandfonline.com/koni.

 Supplemental data for this article can be accessed [here](#).

© 2018 The Author(s). Published by Taylor & Francis.

This is an Open Access article distributed under the terms of the Creative Commons Attribution-NonCommercial-NoDerivatives License (<http://creativecommons.org/licenses/by-nc-nd/4.0/>), which permits non-commercial re-use, distribution, and reproduction in any medium, provided the original work is properly cited, and is not altered, transformed, or built upon in any way.

Here we used the $p53^{+/-}WASp^{-}$ and $p53^{+/-}WASp-XLN$ mice to test if WASp mutations synergize with p53 in carcinogenesis. Using this model, we provide evidence for that WASp deficiency is associated with earlier onset of tumors. In contrast, gain-of-function XLN mutations in WASp led to later onset of tumors.

Materials and methods

Mice

Mice were bred and housed at animal facility of the Department of Microbiology Tumor and Cell biology at Karolinska Institutet under defined pathogen-free conditions. The $WASp^{-}$ and the $WASp-XLN$ ($WASp-I296T$ and $WASp-L272P$) mice were backcrossed to the C57BL/6 (B6) background for at least 8 generations. $Trp53tm1Brd$ ($p53^{-/-}$) mice¹⁸ were bred with the $WASp$ mutant mice to generate $p53^{+/-}WASp^{-}$, $WASp-XLN$, and $p53^{+/-}WASp^{+}$ mice as littermate controls. Twenty eight male $p53^{+/-}WASp^{+}$, 14 $p53^{+/-}WASp^{-}$, 16 $p53^{+/-}WASp-XLN$ (10 $p53^{+/-}WASp-I296T+6$ $p53^{+/-}WASp-L272P$), and 9 $p53^{+/+}WASp^{+}$ mice were sublethally irradiated with a single exposure of 4 Gy at a median age of 20 weeks (14–32 weeks) of age. All animal experiments were performed after approval from the local ethical committee (the north Stockholm district court, Dnr 272/13).

Histopathological examination of mice

Mice were sacrificed when they developed visible tumors, showed a severe weight loss, and/or showed signs of severe discomfort. A small number of mice died spontaneously with no early indication of deterioration of their health. Spleen, liver, lymph nodes, thymus, or sternum were collected during autopsy and tissues fixed in 4% neutral buffered formaldehyde solution (Sigma-Aldrich). Tissues were routinely processed, paraffin embedded, and 4 μ m sections were mounted on glass slides, deparaffinized and hematoxylin-eosin stained. For immunohistochemistry, sections were mounted on charged glass slides and deparaffinized. Following heat-induced epitope retrieval (HIER) at pH9 sections were incubated with monoclonal rabbit anti F4/80 (macrophage marker; dilution 1:100, clone SP115, Abcam), or monoclonal rabbit anti CD3 (T-cell marker; dilution 1:200, clone SP7, Thermo Scientific) and visualized by Leica Bond polymer refine detection on a Leica Bond RXm staining platform. For detection of B-cells, sections were heated for 40 min in citrate buffer (pH 6), manually incubated overnight with polyclonal goat anti Pax5 (dilution 1:2500; C-20, Santa Cruz), detected using rabbit-anti-goat (1:300, Dako) and visualized using Vectastain ABC and ImmPACT DAB kits (Vector Laboratories) according to the manufacturer's instructions, and countersained with hematoxylin. Stained sections were reviewed by a veterinary pathologist (R.K.).

Flow cytometry

To determine early onset changes of the cellularity in peripheral blood, blood samples were collected at regular intervals up to

15 weeks after irradiation and during autopsy. To quantify the amount of hematopoietic cells, AccuCheck counting beads (Invitrogen by Thermo Fisher Scientific) were added to heparin treated blood samples before staining. Red blood cells were lysed with hypotonic salt. For other tissues, single-cell suspensions of spleen, liver, thymus, and tumor were prepared, red blood cells were lysed, and cells were labeled with fluorescently conjugated anti-mouse antibodies: CD45 (APC-Cy-7; hematopoietic cells), CD3 (PE; T lymphocytes), B220 (FITC; B lymphocytes), CD11b (Pacific Blue; myeloid cells) and Ly6G (PE; neutrophils). Spleen suspensions and peripheral blood samples of mice were stained with CD3e (PE; T lymphocytes), CD19 (APC-Cy-7; B lymphocytes), CD11b and CD34 (FITC; hematopoietic progenitor cells). To block Fc receptor binding, purified anti-CD16/32 was added to the staining solutions. All antibodies were purchased from BioLegend. Dead cells were detected by using 4',6-Diamidino-2-phenylindol (DAPI) and excluded from the gating. Flow cytometric analyses were performed on an LSRFortessa X-20 using FACSDiva software (Becton Dickinson). Data were analyzed using the FlowJo software (Tree Star, Inc.).

Tumor killing assay

The YAC-1 T cell lymphoma cell line was stable transfected with Luciferase-pcDNA3.²⁴ Luciferase-pcDNA3 was a gift from William Kaelin (Addgene plasmid #18,964). Natural killer (NK) cells were purified from spleens of poly I:C injected mice with negative selection (Miltenyi Biotec). YAC-1-luciferase cells were co-incubated with NK cells in various ratios for 6h in 96 well plates. Luciferase activity was measured in lysed cells with luciferin substrate (Sigma-Aldrich). NK cell killing activity was calculated as percentage of luciferase signal of the total signal of YAC-1 cells in the absence of NK cells.

In vitro neutrophil differentiation

Neutrophil differentiation in liquid culture was performed as described by Gupta et al.²⁵ Hematopoietic progenitors and stem cells were purified from bone marrow suspension with negative selection (Stemcell Technologies). Equal cell density of each genotype was cultured for 3 days in the presence of SCF and IL-3. 50,000 cells were plated in each well of 96 well plates, and supplemented with SCF, IL-2, and G-CSF to induce promyelocyte differentiation for 2 days. Where indicated, samples were irradiated at day 3 with 1 Gy using X-ray. At day 5, cell numbers were determined with AccuCheck counting beads using flow cytometry.

Statistical analysis

Data were analyzed and processed using Prism 7.0 software (GraphPad Software). Survival curves were generated by using the Kaplan-Meier method and compared by Gehan-Breslow-Wilcoxon test. Laplace regression²⁶ was used to estimate the differences in the 10th and 20th percentiles of survival time between $p53^{+/-}WASp^{\pm}$ and $p53^{+/-}WASp^{-}$ or $p53^{+/-}WASp-XLN$ groups.

Results

To evaluate tumor incidence, onset, and cell origin, we bred WASp mutant mice with $p53^{-/-}$ mice to generate $p53^{+/-}$ WASp⁺ (28 mice), $p53^{+/-}$ WASp⁻ (14 mice), and $p53^{+/-}$ WASp-XLN mice (16 mice). To induce genotoxic stress, these mice were sublethally irradiated and followed for 24 weeks. Two weeks after irradiation, the blood B and T lymphocyte count dropped in all genotypes and then recovered at week 4 (Figure 1A). $p53^{+/-}$ WASp⁺ rebounded to a higher lymphocyte count than $p53^{+/-}$ WASp⁻ (WT). $p53^{+/-}$ WASp⁻ mice had significantly lower number of blood T and B lymphocytes than the $p53^{+/-}$ WASp⁺ control mice during the whole period of monitoring, including the time before irradiation (Figure 1A). Myeloid cell number in blood did not drop (Figure 1B left panel), however 2 weeks after irradiation 2/16 $p53^{+/-}$ WASp-XLN mice (12.5%) showed a sharp temporary expansion of the myeloid compartment (Figure 1B right panel). The expanded cells in these two $p53^{+/-}$ WASp-XLN mice represented a 7–9 fold increase in monocytes (CD11b⁺SSC^{lo} cells) and 11–20 fold expansion of neutrophils (CD11b⁺SSC^{hi} cells). Although this cell expansion occurred stochastic *in vivo*, *in vitro* bone marrow myeloid cultures of WASp-XLN (WASp-I296T and WASp-L272P) consistently showed higher rate of proliferation than WASp⁺ control cultures, regardless of p53 genotype or irradiation (Fig. S1A). Deaths in the cohort started at 6 weeks after irradiation and through the whole 24 week period, the survival curve shows that

$p53^{+/-}$ WASp⁻ mice had lower survival rate when compared to $p53^{+/-}$ WASp⁺ and $p53^{+/-}$ WASp-XLN mice (Figure 1C).

Mice were sacrificed upon detection of a palpable tumor, upon severe weight loss, signs of severe suffering, or when reaching the end point set at 24 weeks. Terminal events during the experiment were initially categorized by macroscopic features and light microscopy on H&E sections. The presence of a visible (sub) cutaneous tumor (Figure 2A) with spindle shape cells showing frequent mitoses (Figure 2B left panel) was classified as sarcoma (Table 1A). Severely enlarged thymus (Figure 2A middle panel) or splenomegaly with extensive lymphoid infiltration of liver (Figure 2B right panel) and lymphoid organs was classified as lymphoma (Table 1B). Six other cases of deaths showed signs of both lymphoid and myeloid proliferation (Table 1C) or there was no information to establish cause of death (Table 1D).

Examination of body weight revealed that mice with lymphoma and the uncharacterized cohort of mice showed marked weight loss shortly before death (Figure 2C). Mice with sarcomas maintained their normal body weights (Figure 2C). Similarly, mice with lymphoma and the uncharacterized cohort had splenomegaly while sarcoma mice had relatively small spleens at the endpoint (Figure 2D). Plotting deaths over time showed that sarcomas were rising earlier while lymphomas appeared later (Figure 2E).

Immune phenotyping showed that a large proportion (more than 50%) of spindle cells in sarcomas were positive for F4/80 (macrophage, myeloid lineage) (Figure 3A). This

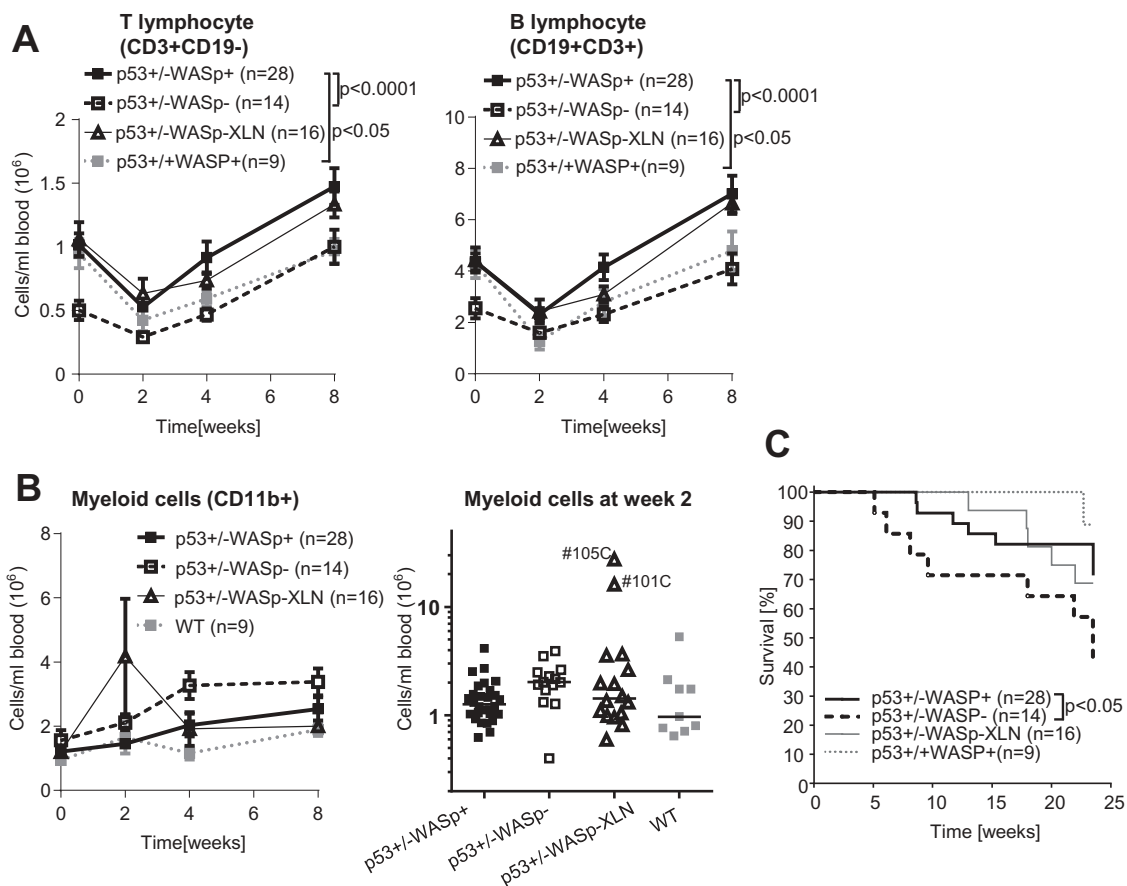


Figure 1. Blood leucocyte counts and survival rate in the $p53^{+/-}$ WASp mutant tumor model. Blood lymphocyte (A) and (B) myeloid cell counts were determined with flow cytometry for 8 weeks after irradiation. Two-way ANOVA and Bonferroni's multiple comparison test. Mean \pm SEM. (B right panel: median myeloid count) (C) Kaplan-Meier survival curve of $p53^{+/-}$ WASp⁺, $p53^{+/-}$ WASp⁻, $p53^{+/-}$ WASp⁻ XLN, and $p53^{+/-}$ WASp⁺ mice. (p value: Gehan-Breslow-Wilcoxon test).

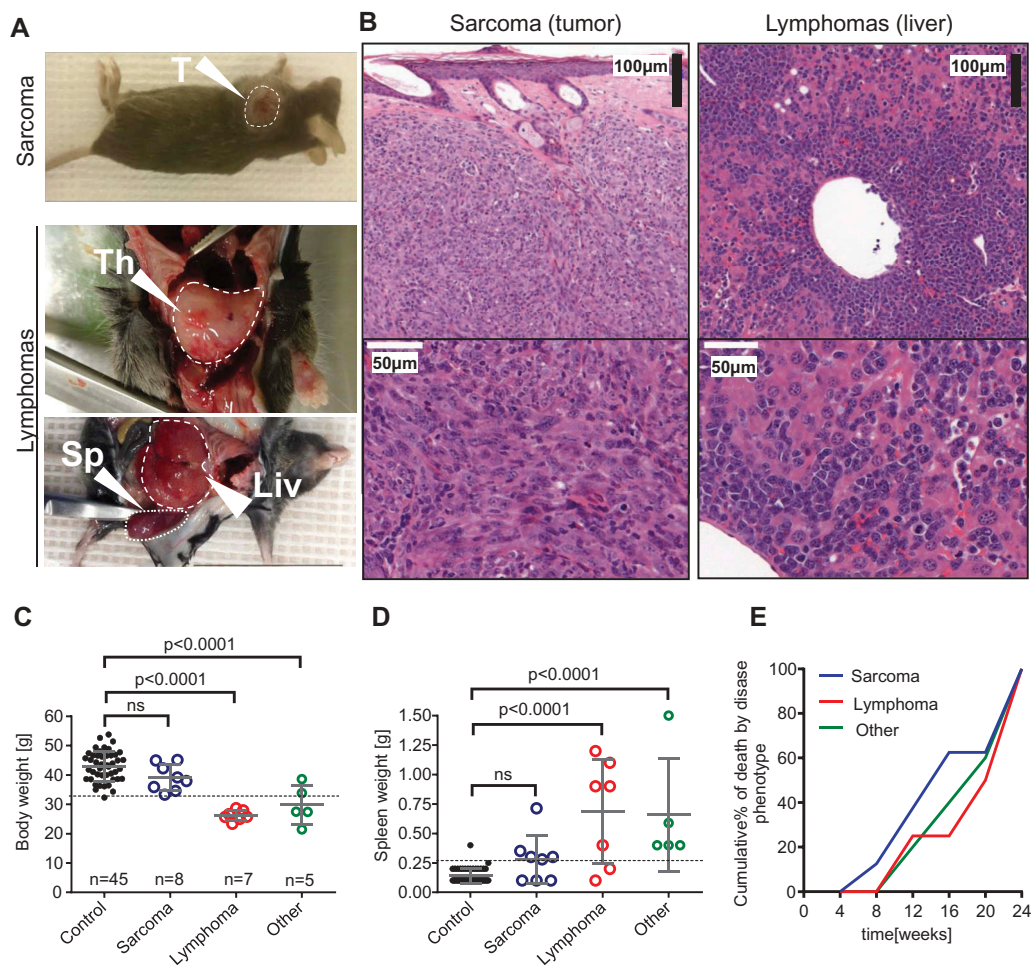


Figure 2. Phenotypical features of malignancies in the $p53^{+/-}$ irradiation model. (A) Sarcomas (upper panel) were initially identified as visible tumors on exteriors. Lymphomas (lower panels) were recognized in animals showing severe weight loss, enlarged thymus or a combination of extreme splenomegaly and other microscopic features. T: tumor; Th: thymus; Sp: spleen; Liv: liver. (B) Hematoxylin-eosin stained tissue sections from sarcoma (#135A left panel) and lymphoma (#65B right panel). (C) Body weight before sacrificing in control (survived until endpoint) mice vs. mice with various pathology and (D) spleen weight at endpoint in control (survived until endpoint) mice vs. mice with various pathology. ANOVA and Bonferroni's multiple comparison test. Mean \pm SD. (E) Cumulative % of tumor deaths was calculated by binning the frequencies of deaths into 4 weeks periods.

phenotype is consistent with histiocytic sarcoma, a frequent tumor in C57BL/6 mice that can be triggered with chronic low-dose irradiation.²⁷ FACS analysis of the tumor cell suspension indicated a large proportion of hematopoietic (CD45+) cells in the tumor mass, which mostly came from the myeloid lineage and contained neutrophils when the tumor was ulcerating (Figure 3B and Table 1A).

In the cases diagnosed as lymphomas, tumor cells dominating in lymphoid tissues and liver stained positive for the pan T cell marker CD3 (Figure 3C, D). Interestingly, spleens frequently contained lineage negative (CD3-CD19-CD11b-) cells with lymphocyte morphology possibly due to downregulation of specific surface markers on the neoplastic cells. The third group of mice showed mild (#117C and #111A) and severe (#44C, 114A) disease of mixed proliferation of hematopoietic cells. Mice #44C and #114A were sacrificed due to life threatening rapid weight loss. They exhibited scattered infiltration of leukocytes in liver mostly with myeloid but occasional lymphoid infiltrates with morphology suggestive of autonomous proliferation (Figure 3E, F). Mice #117C and #111A were selected in the disease cohort due to

splenomegaly and hematopoietic liver infiltrates. Immune cell clusters in these mice showed perivascular location, consistent with histological changes in aged liver that is associated with carcinogenesis.²⁸

When compiling data, we found that although the frequency of deaths was almost double in $p53^{+/-}$ WASp⁻ mice compared to $p53^{+/-}$ WASp⁺ mice, the distribution of various cancer types was similar between all $p53^{+/-}$ mice (Figure 4A). One out of 9 irradiated WT ($p53^{+/+}$ WASp⁺) control mice developed histiocytic sarcoma. In contrast, lymphomas only occurred in $p53^{+/-}$ mice (Figure 4A). The death rate at 12 weeks was 10.6% of $p53^{+/-}$ WASp⁺ mice, 28.6% of $p53^{+/-}$ WASp⁻ mice (21.4% confirmed malignant), and 0% of $p53^{+/-}$ WASp-XLN mice and $p53^{+/-}$ WASp[±] mice (Figure 4B). The death rate of confirmed malignancies (Figure 4A, indicated in bold font) during 24 weeks was 35.7% of $p53^{+/-}$ WASp⁻ mice and 25.0% of $p53^{+/-}$ WASp[±] mice. This suggests that the onset of tumor development differed between the groups. To compare the onset of deaths in each group, we calculated the survival time and confidence intervals at 10th and 20th survival percentiles (in each cohort corresponding to 90% and 80%

Table 1. Malignancies in the p53^{+/-} irradiation model.

No.	p53 genotype	WASp genotype	Death after irradiation (weeks)	Histology	Macroscopically ulcerating	Splenomegaly	Tumor infiltration of CD45+ (FACS)
A) Spindle cell tumors							
46B	+/-	+	9	Cystic hair follicle dilatation with large numbers of F4/80+ spindle shaped atypical cells in surrounding dermis	NO	YES	N/A
89C	+/-	+	13	Spindle tumor, malignant, NOS; up to 8 mit/40x. Ulcerated. Extensive F4/80 positivity in spindle cell tumor area.	YES	NO	low myeloid
135A	+/-	+	24	Spindle tumor, malignant, NOS; up to 10 mit/40x. Ulcerated. Extensive F4/80 positivity in spindle cell tumor area.	YES	YES	N/A
87A	+/-	-	6	Spindle tumor, malignant, NOS. Neutrophils are present in the necrotic area, but the tumor is not heavily infiltrated.	YES	YES	high myeloid
89A	+/-	-	8	Subcut. abscess overlying lymphnode. Marked F4/80+ spindle cell proliferation in surroundings, neovascularisation. Neutrophils are associated with the abscess with puss.	NO	YES	high myeloid SP,BL: CD11b exp.
83B	+/-	XLN (I296T)	22	Spindle tumor, malignant, NOS; up to 6 mit/40x. Ulcerated. Extensive F4/80 positivity in spindle cell tumor area. Neutrophils are abundant in the tumor mass even far from the ulceration.	NO	YES	low myeloid+
105C	+/-	XLN (L272P)	13	Spindle tumor, malignant, NOS; up to 5 mit/40x. Extensive F4/80 positivity in spindle cell tumor area. Neutrophils are rare and they are not appear to be the integral part of tumor mass.	NO	NO	Low SP: CD11b exp.
49B	+/+	+	23	Spindle tumor, malignant, NOS; up to 5 mit/40x. Extensive F4/80 positivity in spindle cell tumor area.	NO	NO	N/A
No.	p53 genotype	WASp genotype	Death after irradiation (weeks)	Histology	Enlarged thymus	Splenomegaly	Hematopoietic infiltration (FACS)
B) Lymphomas							
119A	+/-	+	24	N/A	YES	YES	
123A	+/-	+	9	Neoplastic, lymphoid infiltr. of BM, LN, SPL, liver and lung	NO	YES	LIV: High T cell infiltr. BL: T norm, B lymphopenia
124A	+/-	+	12	Hematopoietic neoplasm	NO	YES	LIV: T cell SP,BL: T cell exp.
78A	+/-	-	24	Lymphoma	YES	YES	LIV: T cell exp.
118A	+/-	-	22	Lymphoma	YES	NO	LIV: T cell exp. SP:CD34+ exp.
65B	+/-	XLN(I296T)	18	High grade lymphoblastic lymphoma	YES	YES	
84B	+/-	XLN(I296T)	20	N/A	YES	N/A	
101C	+/-	XLN(L272P)	18	N/A	YES	NO	
No.	p53 genotype	WASp genotype	Death after irradiation (weeks)	Histology	Cause of death	Splenomegaly	Hematopoietic infiltration (FACS)
C) Mixed hematopoietic proliferation							
44C	+/-	+	15	LIV: enlarged, white dotted LIV, SP, BM: hematopoietic expansion LIV: Large numbers of F4/80+ cells Disseminated histiocytic neoplasm?	Severe weightloss	YES	LIV: T cell (CD3+) and myeloid (CD11b+) infiltration SP: T,B compartments are replaced by lin-(CD3-CD19-CD11b-) cells
117C	+/-	+	24	Pre-neoplastic? SP,BM: myeloid proliferation	EP	YES	BL: T,B lymphopenia LIV: T cell (CD3+) and myeloid (CD11b+) infiltration SP: norm.
111A	+/-	-	24	Pre-neoplastic? SP,LIV: mixed proliferation of hematopoietic components, probably lymphocytes and macrophages. SP,BM: myeloid proliferation	EP	YES	Myeloid infiltration in liver SP: T,B compartments are replaced by lin-(CD3-CD19-CD11b-) cells
114A	+/-	-	10	LIV, LN: mainly lymphoblastic proliferation with myeloid components	Severe weightloss	YES	LIV (pale col.): High myeloid (CD11b+) expansion. T,B exp. SP: T,B compartments are replaced by lin-(CD3-CD19-CD11b-) cells BL (pale color): very high myeloid counts, T,B lymphopenia
No.	p53 genotype	WASp genotype	Death after irradiation (weeks)	Histology	Cause of death	Splenomegaly	Hematopoietic infiltration (FACS)
D) Unknown							
101A	+/-	-	18	Large abscess on skin; reactive expansion of myeloid lineage?	Prolif.	YES	
153A	+/-	-	5	N/A	Severe weightloss	N/A	

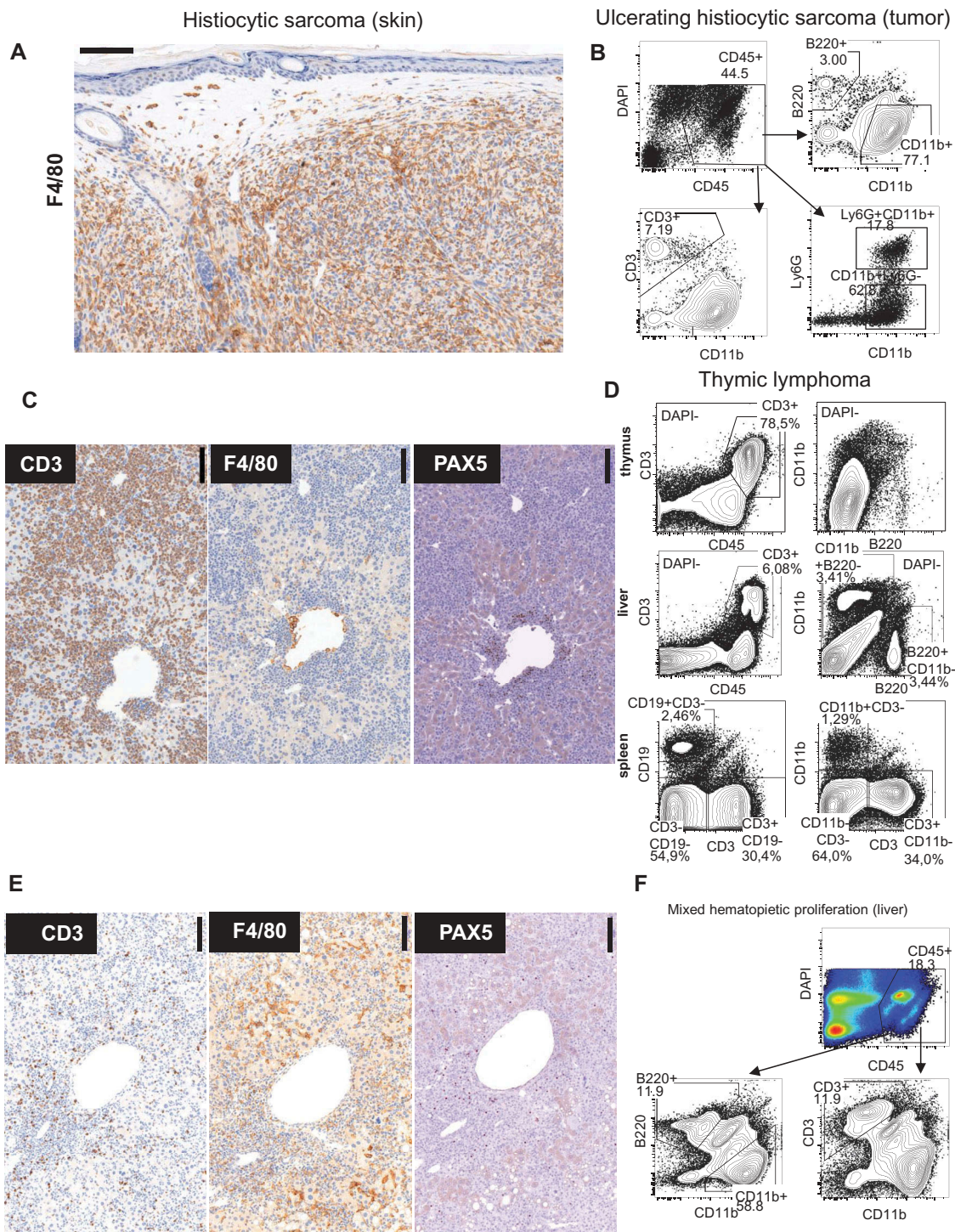


Figure 3. Immunophenotypic features of malignancies in $p53^{\pm/-}$ irradiation model. (A) F4/80 immunohistochemistry of subcutaneous tumor. (#135A) (B) FACS analysis of large ulcerating tumor. (#87A) (C) Immunohistochemistry of liver in lymphoma with the indicated antibodies. (#124A). (D) FACS analysis of thymus, liver, and spleen in mouse with thymic lymphoma. (#78A) (E) Immunohistochemistry of liver of mouse with severe mixed hematopoietic proliferation. (#44C). (F) FACS Liver (#114A).

live mice, respectively) from Figure 1C. We found that $p53^{\pm/-}$ WASp⁻ mice had earlier onset of deaths when compared to $p53^{\pm/-}$ WASp[±] mice (Figure 4C top panel). In contrast, $p53^{\pm/-}$ WASp-XLN mice had had later onset of deaths when compared to $p53^{\pm/-}$ WASp[±] mice (Figure 4C bottom panel) in these survival percentiles.

The finding that there was no dominance of a specific tumor in the different WASp genotypes, suggested that

altered tumor surveillance due to WASp mutations may contribute to the tumor incidence. To test tumor cell killing, NK cells were incubated with YAC-1 lymphoma cells expressing luciferase and the loss of luciferase signal quantified. WASp deficient NK cells showed reduced killing of YAC-1 lymphoma cells when compared to wildtype NK cells (Figure 4D-E) whereas WASp-XLN NK cells showed increased killing of YAC-1 lymphoma cells (Figure 4D-E).

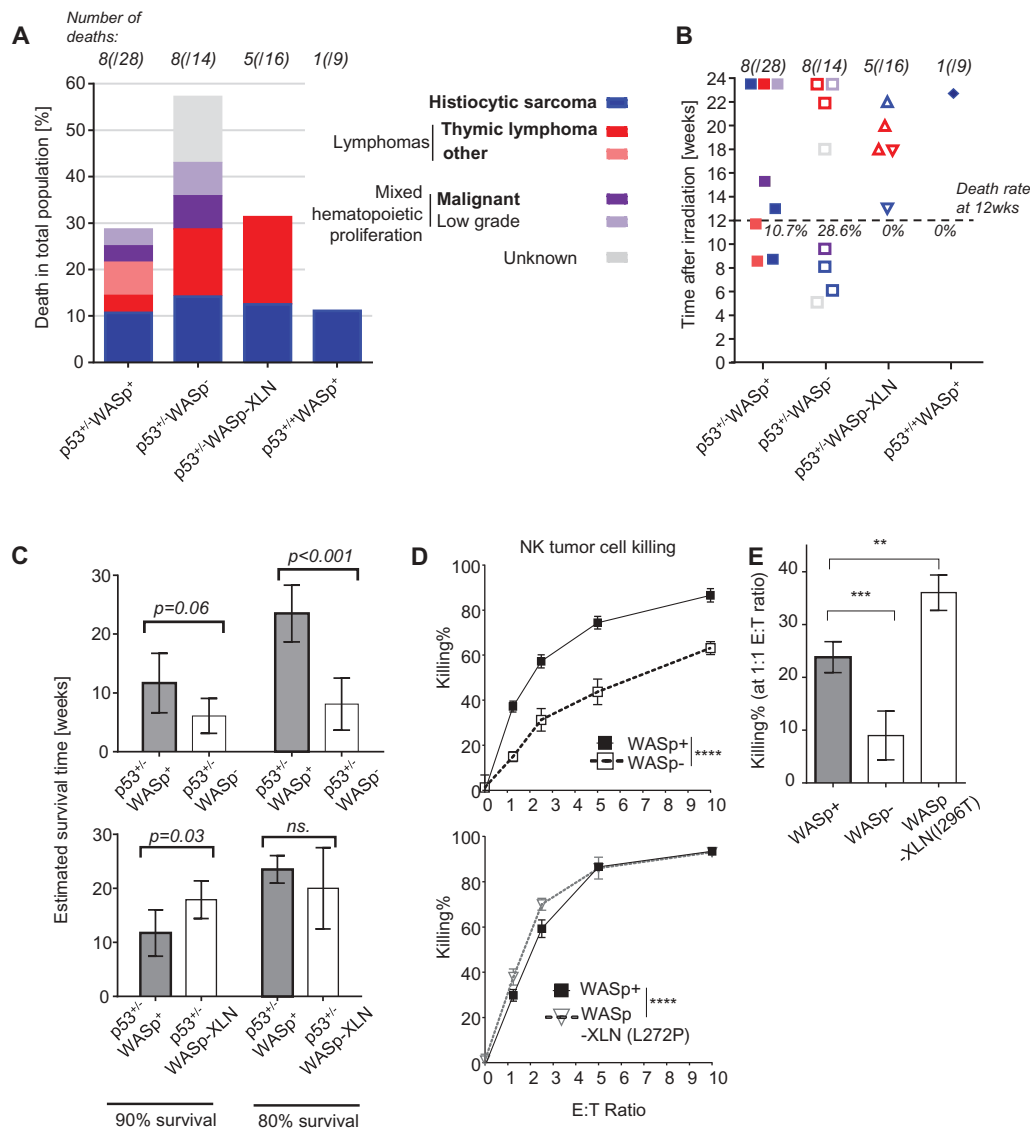


Figure 4. Frequency of deaths in $p53^{+/-}$ -WASp mutant tumor model. (A) Frequency of deaths per genotype. Bold text indicates malignant cause of death. (B) Time of death after irradiation. Causes of death are color coded as on Figure 4A. (C) Survival time and 95% confidence intervals at 10th and 20th survival percentiles was calculated from the Figure 1C survival curve with Laplace regression. (D, E) Killing of YAC-1-luciferase tumor cells by NK cells was quantified with chemiluminescence. Mean \pm SD; Two-way ANOVA (D) and ANOVA with Bonferroni's multiple comparisons test (E). **: $p \leq 0.01$, ***: $p \leq 0.001$, ****: $p \leq 0.0001$.

Together, this data suggests that reduced tumor immune surveillance by WASp deficient NK cells contribute to poor survival of $p53^{+/-}$ -WASp $^{-}$ mice and on the contrary, that overactive WASp in WASp-XLN NK cells lead to delayed tumor onset of $p53^{+/-}$ -WASp-XLN mice.

Discussion

Together, we describe a spontaneous murine tumor model where sub-lethally irradiated $p53^{+/-}$ -WASp mutant mice developed solid tumors, lymphoid malignancies, and other pathological conditions. Although predominant in WAS patients, no B cell lymphomas developed in the $p53^{+/-}$ -WASp $^{-}$ colony. Targeted deletion of *p53* gene expression results an earlier occurrence of thymic lymphomas and only a small percentage of *p53*-deficient mice succumb to B cell lymphomas.²⁹ If *p53* is conditionally targeted in the B cell lineage, a very late onset of B cell lymphomas occurs and these lack immunoglobulin

translocations²⁹. Importantly, we show here that WASp deletion itself does not alter the T cell lymphoma propensity bias of *p53* mutant mice toward B cell malignancies. This suggests that WAS patient lymphomas do not stem from intrinsic failure of WAS B cells to suppress tumor transformation but rather an external factor such as the overall tumor surveillance defect of the WASp deficient immune system. We show here that WASp deficient NK cells have reduced capacity to kill YAC-1 lymphoma cells. B cell lymphoma predominance in WAS patients is likely to originate from oncogenic transformation of EBV infection or long exposure – due to long lifespan – of human B cells to proliferation signals. Noticeably, $p53^{+/-}$ -WASp $^{-}$ mice had a significantly decreased survival rate and they developed various early onset malignancies sooner than $p53^{+/-}$ -WASp $^{+}$ mice. It has previously been shown that WASp $^{-}$ mice bred to tumor susceptible *Cdkn2a* knockout background also show earlier death and poor rejection of injected B16 melanoma cells when compared

to WASp⁺ mice.³⁰ Poor tumor survival and rejection capacity is at least partly caused by reduced tumor surveillance by WASp⁻ NK cells and cytotoxic T cells as we and others have shown.³⁰⁻³⁴ It is therefore likely that poor tumor prognosis in p53^{+/-}WASp⁻ could be explained by aberrant tumor surveillance by WASp⁻ cytotoxic cells.

Similarly to p53^{+/-}WASp⁻ mice that do not develop B cell lymphomas, p53^{+/-}WASp-XLN mice do not develop AML. Severe congenital neutropenias (SCNs), such as XLN are considered pre-leukemic conditions due to bone marrow failure. Although the exact pathophysiology of XLN is not known yet it is likely that AML emerges in XLN patients due to chronic neutropenia and the occasional G-CSF treatment. XLN mutations have been suggested to cause chromosomal instability due to increased F-actin load in the cytoplasm and elevated cytoplasmic viscosity which mechanically disrupt proper cell division.¹⁶ We found here that WASp-XLN myeloid cells proliferated extensively *in vitro* and that two XLN-WASp mice showed marked myeloid expansion at 2 weeks after irradiation that was quickly resolved. Despite the dysregulated myeloid proliferation, XLN-WASp had late onset tumors. This suggests the myeloid expansion do not lead to transformation *in vivo* using this model. Importantly, p53 only responds to particular types of genotoxic stress and our experiments suggest that chromosomal abnormalities emerging in XLN fail to synergize with p53 deletion.²⁹ In contrast to the p53^{+/-}WASp⁻ colony, the p53^{+/-}WASp-XLN mice developed cancer mostly with late onset leading to delayed mortality. This implies that p53^{+/-}WASp-XLN mice were more resistant against tumor development when compared to p53^{+/-}WASp⁺ mice and that tumor immunosurveillance was not impaired in p53^{+/-}WASp-XLN mice. In fact, WASp-XLN NK cells showed increased killing capacity of YAC-1 lymphoma cells.

WASp mutations compromise the immune system at multiple levels.³⁵ In our model, tumor development depends on the combination of genetic predisposition to DNA mutations by p53 deficiency, environmental stress by gamma radiation, and compromised immune system by WASp mutations. Our results help to understand to multifaceted nature of carcinogenic effects of WASp mutations.

Abbreviations

SD	standard deviation
WAS	Wiskott-Aldrich syndrome
WASp	WAS protein
WT	wild type
XLN	X-linked neutropenia

Disclosure of Potential Conflicts of Interest

No potential conflict of interest was reported by the authors.

Acknowledgments

We thank Tarja Schröder and Agneta Andersson at the Karolinska Institutet core facility for Morphologic Phenotype Analysis to perform histotechnique and immunohistochemistry. We thank Andrea

Discacciati at the Karolinska Institutet Biostatistics Core Facility for biostatistics consultation.

Funding

This work was supported by a postdoctoral fellowship from the Cancer Society to M.K., a postdoctoral fellowship from the Olle Engqvist Byggnästare foundation to M.H., a PhD fellowship from Fundação para a Ciência e a Tecnologia to M.M.S.O., and by research grants from O. E. och Edla Johanssons vetenskapliga stiftelse and the Lars Hierta Memorial Foundation to M.K., Center for Innovative Medicine/ CIMED) to R.K., and Swedish Research Council, Cancer Society, Childhood Cancer Society, Åke Olsson foundation, Bergvall Foundation, King Gustaf V's 80-year Foundation, and Karolinska Institutet to L.S.W. L.S.W. is a Ragnar Söderberg fellow in Medicine.

ORCID

Hannah Wurzer  <http://orcid.org/0000-0001-5816-1286>

References

- Mortaz E, Tabarsi P, Mansouri D, Khosravi A, Garssen J, Velayati A, Adcock IM. Cancers related to immunodeficiencies: update and perspectives. *Front Immunol.* 2016;7:365. doi:10.3389/fimmu.2016.00365.
- Imai K, Morio T, Zhu Y, Jin Y, Itoh S, Kajiwara M, Yata J, Mizutani S, Ochs HD, Nonoyama S. Clinical course of patients with WASP gene mutations. *Blood.* 2004;103:456–464. doi:10.1182/blood-2003-05-1480.
- Sullivan KE, Mullen CA, Blaese RM, Winkelstein JA. A multi-institutional survey of the Wiskott-Aldrich syndrome. *J Pediatr.* 1994;125:876–885. doi:10.1016/S0022-3476(05)82002-5.
- Tran H, Nourse J, Hall S, Green M, Griffiths L, Gandhi MK. Immunodeficiency-associated lymphomas. *Blood Rev.* 2008;22:261–281. doi:10.1016/j.blre.2008.03.009.
- Senapati J, Devasia AJ, David S, Manipadam MT, Nair S, Jayandharan GR, George B. Diffuse large B cell lymphoma in wiskott-Aldrich syndrome: a case report and review of literature. *Indian J Hematol Blood Transfus.* 2014;30:309–313. doi:10.1007/s12288-014-0377-1.
- Du S, Scuderi R, Malicki DM, Willert J, Bastian J, Weidner N. Hodgkin's and non-Hodgkin's lymphomas occurring in two brothers with Wiskott-Aldrich syndrome and review of the literature. *Pediatr Dev Pathol: Off J Soc Pediatr Pathol Paediatric Pathol Soc.* 2011;14:64–70. doi:10.2350/10-01-0787-CR.1.
- Filipovich AH, Mathur A, Kamat D, Shapiro RS. Primary immunodeficiencies: genetic risk factors for lymphoma. *Cancer Res.* 1992;52:5465s–7s.
- Salavoura K, Kolialexi A, Tsangaris G, Mavrou A. Development of cancer in patients with primary immunodeficiencies. *Anticancer Res.* 2008;28:1263–1269.
- Worth AJ, Thrasher AJ. Current and emerging treatment options for Wiskott-Aldrich syndrome. *Expert Rev Clin Immunol.* 2015;11:1015–1032. doi:10.1586/1744666X.2015.1062366.
- Yoshimi A, Kamachi Y, Imai K, Watanabe N, Nakadate H, Kanazawa T, Ozono S, Kobayashi R, Yoshida M, Kobayashi C, et al. Wiskott-Aldrich syndrome presenting with a clinical picture mimicking juvenile myelomonocytic leukaemia. *Pediatr Blood Cancer.* 2013;60:836–841. doi:10.1002/pbc.v60.5.
- Beel K, Cotter MM, Blatny J, Bond J, Lucas G, Green F, Vanduppen V, Leung DW, Rooney S, Smith OP, et al. A large kindred with X-linked neutropenia with an I294T mutation of the Wiskott-Aldrich syndrome gene. *Br J Haematol.* 2009;144:120–126. doi:10.1111/bjh.2008.144.issue-1.
- Devriendt K, Kim AS, Mathijs G, Frints SG, Schwartz M, Van Den Oord JJ, Verhoef GEG, Boogaerts MA, Fryns J-P, You D, et al. Constitutively activating mutation in WASP causes X-linked

- severe congenital neutropenia. *Nat Genet.* 2001;27:313–317. doi:10.1038/85886.
13. Ancliff PJ, Blundell MP, Cory GO, et al. Two novel activating mutations in the Wiskott-Aldrich syndrome protein result in congenital neutropenia. *Blood.* 2006;108:2182–2189. doi:10.1182/blood-2006-01-010249.
 14. Moulding DA, Blundell MP, Spiller DG, White MR, Cory GO, Calle Y, Kempski H, Sinclair J, Ancliff PJ, Kinnon C, et al. Unregulated actin polymerization by WASp causes defects of mitosis and cytokinesis in X-linked neutropenia. *J Exp Med.* 2007;204:2213–2224. doi:10.1084/jem.20062324.
 15. Westerberg LS, Meelu P, Baptista M, Eston MA, Adamovich DA, Cotta-de-Almeida V, Seed B, Rosen MK, Vandenberghe P, Thrasher AJ, et al. Activating WASP mutations associated with X-linked neutropenia result in enhanced actin polymerization, altered cytoskeletal responses, and genomic instability in lymphocytes. *J Exp Med.* 2010;207:1145–1152. doi:10.1084/jem.20091245.
 16. Moulding DA, Moeendarbary E, Valon L, Record J, Charras GT, Thrasher AJ. Excess F-actin mechanically impedes mitosis leading to cytokinesis failure in X-linked neutropenia by exceeding Aurora B kinase error correction capacity. *Blood.* 2012;120:3803–3811. doi:10.1182/blood-2012-03-419663.
 17. Coppe A, Nogara L, Pizzuto MS, Cani A, Cesaro S, Masetti R, Locatelli F, Te Kronnie G, Basso G, Bortoluzzi S, et al. Somatic mutations activating Wiskott-Aldrich syndrome protein concomitant with RAS pathway mutations in juvenile myelomonocytic leukemia patients. *Hum Mutat.* 2018;39:579–587. doi:10.1002/humu.23399.
 18. Donehower LA, Harvey M, Slagle BL, McArthur MJ, Montgomery CA Jr., Butel JS, Bradley A. Mice deficient for p53 are developmentally normal but susceptible to spontaneous tumours. *Nature.* 1992;356:215–221. doi:10.1038/356215a0.
 19. Kemp CJ, Wheldon T, Balmain A. p53-deficient mice are extremely susceptible to radiation-induced tumorigenesis. *Nat Genet.* 1994;8:66–69. doi:10.1038/ng0994-66.
 20. Bouffler SD, Kemp CJ, Balmain A, Cox R. Spontaneous and ionizing radiation-induced chromosomal abnormalities in p53-deficient mice. *Cancer Res.* 1995;55:3883–3889.
 21. Lee JM, Abrahamson JL, Kandel R, Donehower LA, Bernstein A. Susceptibility to radiation-carcinogenesis and accumulation of chromosomal breakage in p53 deficient mice. *Oncogene.* 1994;9:3731–3736.
 22. Zhao Z, Zuber J, Diaz-Flores E, Lintault L, Kogan SC, Shannon K, Lowe SW. p53 loss promotes acute myeloid leukemia by enabling aberrant self-renewal. *Genes Dev.* 2010;24:1389–1402. doi:10.1101/gad.1940710.
 23. Adams CM, Eischen CM. Inactivation of p53 is insufficient to allow B cells and B-cell lymphomas to survive without Dicer. *Cancer Res.* 2014;74:3923–3934. doi:10.1158/0008-5472.CAN-13-1866.
 24. Safran M, Kim WY, O'Connell F, Flippin L, Gunzler V, Horner JW, DePinho RA, Kaelin WG. Mouse model for noninvasive imaging of HIF prolyl hydroxylase activity: assessment of an oral agent that stimulates erythropoietin production. *Proc Natl Acad Sci USA.* 2006;103:105–110. doi:10.1073/pnas.0509459103.
 25. Gupta D, Shah HP, Malu K, Berliner N, Gaines P. Differentiation and characterization of myeloid cells. *Curr Protoc Immunol.* 2014;104:Unit 22F 5.
 26. Bottai M, Zhang J. Laplace regression with censored data. *Biom J Biometrische Zeitschrift.* 2010;52:487–503. doi:10.1002/bimj.200900310.
 27. Lacroix-Triki M, Lacoste-Collin L, Jozan S, Charlet JP, Caratero C, Courtade M. Histiocytic sarcoma in C57BL/6J female mice is associated with liver hematopoiesis: review of 41 cases. *Toxicol Pathol.* 2003;31:304–309. doi:10.1080/01926230390204342.
 28. Singh P, Coskun ZZ, Goode C, Dean A, Thompson-Snipes L, Darlington G. Lymphoid neogenesis and immune infiltration in aged liver. *Hepatology (Baltimore, Md).* 2008;47:1680–1690. doi:10.1002/hep.22224.
 29. Gostissa M, Bianco JM, Malkin DJ, Kutok JL, Rodig SJ, Morse HC 3rd, Bassing CH, Alt FW. Conditional inactivation of p53 in mature B cells promotes generation of nongermline center-derived B-cell lymphomas. *Proc Natl Acad Sci USA.* 2013;110:2934–2939. doi:10.1073/pnas.1222570110.
 30. Catucci M, Zanoni I, Draghici E, Bosticardo M, Castiello MC, Venturini M, Cesana D, Montini E, Ponzoni M, Granucci F, et al. Wiskott-Aldrich syndrome protein deficiency in natural killer and dendritic cells affects antitumor immunity. *Eur J Immunol.* 2014;44:1039–1045. doi:10.1002/eji.201343935.
 31. Orange JS, Roy-Ghanta S, Mace EM, Maru S, Rak GD, Sanborn KB, Fasth A, Saltzman R, Paisley A, Monaco-Shawver L, et al. IL-2 induces a WAVE2-dependent pathway for actin reorganization that enables WASp-independent human NK cell function. *J Clin Invest.* 2011;121:1535–1548. doi:10.1172/JCI44862.
 32. Kritikou JS, Dahlberg CI, Baptista MA, Wagner AK, Banerjee PP, Gwalani LA, Poli C, Panda SK, Kärre K, Kaech SM, et al. IL-2 in the tumor microenvironment is necessary for Wiskott-Aldrich syndrome protein deficient NK cells to respond to tumors in vivo. *Sci Rep.* 2016;6:30636. doi:10.1038/srep30636.
 33. De Meester J, Calvez R, Valitutti S, Dupre L. The Wiskott-Aldrich syndrome protein regulates CTL cytotoxicity and is required for efficient killing of B cell lymphoma targets. *J Leukoc Biol.* 2010;88:1031–1040. doi:10.1189/jlb.0410197.
 34. Ishihara D, Dovas A, Hernandez L, Pozzuto M, Wyckoff J, Segall JE, Condeelis JS, Bresnick AR, Cox D. Wiskott-Aldrich syndrome protein regulates leukocyte-dependent breast cancer metastasis. *Cell Rep.* 2013;4:429–436. doi:10.1016/j.celrep.2013.07.007.
 35. Thrasher AJ, Burns SO. WASP: a key immunological multitasker. *Nat Reviews Immunol.* 2010;10:182–192. doi:10.1038/nri2724.